

## Preparation, Characterization, and Biological Activity of La(III), Nd(III), Er(III), Gd(III), and Dy(III) Complexes with Schiff Base Resulted from Reaction of 4-Antipyrinecarboxaldehyde and 2-Aminobenzothiazole

Kawther Adeeb Hussein<sup>1\*</sup>, Naser Shaalan<sup>2</sup>, Aliaa Khauon Lafta<sup>3</sup>, and Janan Majeed Al Akeedi<sup>4</sup>

<sup>1</sup>Department of Chemistry, College of Science, Al-Nahrain University, Jadria, Baghdad 10072, Iraq

<sup>2</sup>Department of Chemistry, College of Science for Women, University of Baghdad, Baghdad 10071, Iraq

<sup>3</sup>Iraqi Center for Cancer and Medical Genetics Research, Mustansiriyah University, Baghdad 10052, Iraq

<sup>4</sup>Department of Medical Laboratory Techniques, University Al-Farabi, Baghdad 10022, Iraq

\* **Corresponding author:**

email: kawther.adeeb@nahrainuniv.edu.iq

Received: July 25, 2023

Accepted: October 27, 2023

DOI: 10.22146/ijc.87262

**Abstract:** The research includes the preparation of several complexes of the internal transition elements lanthanide ( $Ln = La, Nd, Er, Gd, \text{ and } Dy$ ) containing the 4f shell, with Schiff bases resulting from condensation reactions between 4-antipyrinecarboxaldehyde and 2-aminobenzothiazoles. Schiff's base was identified using FTIR spectra, UV-vis spectroscopy, elemental microanalysis CHNSO, nuclear magnetic resonance, mass spectrometry, and TGA thermal analysis. The complexes were studied and identified with elemental microanalysis CHNSO, FTIR spectroscopy, UV-vis spectroscopy, TGA thermal analysis, conductivity measurement, and magnetic sensitivity. The result showed that these complexes were classified as homogeneous bidentate complexes with the general formula of  $[Ln_2(L)_2(NO_3)_6] \cdot 6H_2O$ . The physical measurements indicated that the prepared complexes are non-electrolyte and paramagnetic. Some compounds prepared in vitro were evaluated for their antibacterial activity against four types of pathogenic strains *Staphylococcus aureus*, *Bacillus subtilis*, *Escherichia coli*, and *Klebsiella pneumonia*, and using the agar disc spreading method for the evaluation. The results showed that some of these complexes have good antibacterial activity compared to the biological activity of the ligand. Also, the biological activity of Schiff's base and the prepared complexes were evaluated against three types of fungi (*Candida albicans*, Tropical fungi, and Scandal fungi), and they showed great activity against the prepared complexes.

**Keywords:** 4-antipyrinecarboxaldehyde; biological activities; lanthanide complexes; Schiff bases

### ■ INTRODUCTION

Recently, there has been increased interest in the chemistry of the lanthanide inner transition elements and their chemical law:  $ns(n-1)d(n-2)f$ . These elements have a category located at the bottom of the periodic table, and they include elements with atomic numbers starting from 57–71, which are the lanthanides and start with lanthanum, followed by 14 elements with the 4f shell called the lanthanide elements [1-3]. Consisting of rare-earth elements, each element in the lanthanide series has

an  $f$  orbital that is either partially or completely filled with electrons, while the outermost orbital is unoccupied [4]. In their combinations, these elements go beyond the (III) oxidation state, and in some of them, the (II) and (IV) oxidation states show up. The only stable state for lanthanum, gadolinium, and lutetium ion is (III). This is because it is the same as the 4f orbital being empty, half-full, and full [5-6]. The lanthanides differ chemically from the elements in the major groups of the periodic table as well as the intermediate metals.

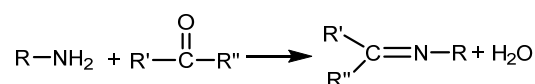
This difference is due to the nature of the sub-layer and what is within it. These orbitals are located inside the atom and covered by electrons in the  $4d$  and  $5p$  orbitals. For this reason, the chemical properties of these elements depend on their size, which increases with an increasing atomic number [7].

Lanthanides are often mixed with other metals to make them harder and stronger. Cerium, which combines with some of the other elements in this group, is the main element used for this reason. In the oil business, these minerals are also used extensively to refine crude oil. Erbium and other lanthanides are also used in night vision cameras, lasers, phosphors, and visual devices [8-9]. Lanthanides possess numerous scientific and economic applications. Their compounds, for instance, are utilized as catalysts in producing petroleum and synthetic goods. Additionally, lanthanides are applied in manufacturing lamps, lasers, magnets, phosphors, movie projectors, and screens that enhance the intensity of X-rays [10]. When light lanthanides are added to a mixed rare earth alloy termed (Mischmetal), the result is extremely combustible. Use iron spray to turn flint stones into lighter tinder. When more than one Mischmetal is added to low alloy steels, the material gains strength and is easier to work with. Even though most metals shine brightly when first cut, they quickly lose their luster when exposed to air; this is especially true of the transition metals (Ce, La, and Eu), which react with water slowly at room temperature but rapidly when heated [11-12].

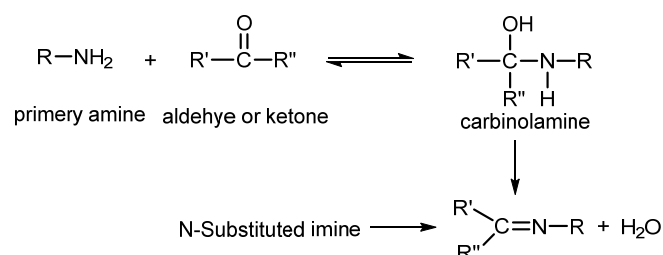
Because of their high electronegativity, lanthanides exhibit the following reactions: they quickly disintegrate in acids and oxidize in damp air. The reaction with oxygen is slow at room temperature, but it can ignite between 150 and 200 °C, react with halogens when heated, and react with sulfur, hydrogen, carbon, and nitrogen when heated as well [13-14]. Lanthanides display a defining characteristic as silvery white metals that rapidly undergo oxidation upon exposure to air [15]. The increase in atomic number results in a slight increase in the material's hardness. As one moves over the period from left to right (which corresponds to an increase in atomic number), the radius of each lanthanide(III) ion gradually decreases [16]. This is called lanthanide contraction, and it means

that the lanthanides have high melting and boiling points. When it comes into contact with water, it gives off hydrogen ( $H_2$ ) slowly when it is cold and quickly when it is hot [17]. Lanthanides are often connected to water due to their potent ability to act as powerful reducing agents. At high temperatures, the compounds of rare earth elements typically display ionic properties. In addition, a significant number of these components possess a remarkable propensity to spontaneously ignite and generate vigorous combustion [18-19]. Most rare earth compounds are highly magnetic. Many rare earth compounds glow brightly under ultraviolet light. Lanthanide ions tend to be faint colors caused by weak, narrow, and inhibited optical transitions [20-21].

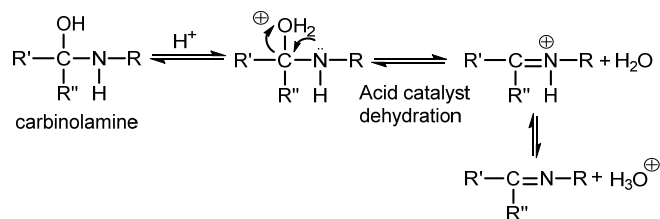
Schiff's bases are nitrogenous chemicals that are similar to aldehydes and ketones but have a  $-C=N-$  group instead of a carbonyl group. Typically, they are synthesized by combining a primary amine with an aldehyde or ketone (Scheme 1) [22]. The alkyl or aryl group (R, R', R'') can serve as Schiff's bases. Schiff bases that contain aryl groups are known for their enhanced stability and ease of preparation. However, Schiff bases obtained from aliphatic aldehydes are more prone to polymerization and are generally regarded as less stable. On the other hand, aromatic aldehydes with multiple links to the aromatic ring are more stable [23]. The reaction of forming Schiff bases from aldehydes or ketones is a reversible reaction, and the reaction generally occurs under acidic or basic conditions as a catalyst or through heating, as shown in Scheme 2 [24].



**Scheme 1.** General reaction of Schiff base formation



**Scheme 2.** The stepwise reaction of Schiff base formation



**Scheme 3.** The mechanism of the Schiff base reaction

The reaction is typically finalized by isolating the end product, eliminating water, or both. In both acidic and basic solutions, numerous Schiff bases can decompose back into their constituent aldehydes or ketones, along with the corresponding elemental amine [25]. Another subject related to nucleophilic addition to the carbonyl group is the mechanism of the Schiff base reaction. The amine acts as the nucleophile in this case. During the initial step of the process, the amine undergoes a reaction with either an aldehyde or a ketone, resulting in the formation of a precarious compound known as carbinolamine. This compound is the result of a nucleophilic addition reaction. When an acid or base is used as a catalyst, the carbinolamine alcohol undergoes dehydration and loses a water molecule, as demonstrated in Scheme 3 [26-27]. The defining step of the Schiff base reaction is usually the loss of water. The acid concentration should not be too high because the amine used is considered a base and when it is purified, it becomes non-nucleophilic and no carbonyl alcohol is formed. Therefore, the preparation of many Schiff bases is preferably done in a moderately acidic condition [28]. The research aims to prepare a new ligand and form complexes through its interaction with the salts of the lanthanide elements, their characterization, and a biological activity study.

## ■ EXPERIMENTAL SECTION

### Materials

The study utilized reagents and chemicals, such as 4-antipyrinecarboxaldehyde (97%), 2-aminobenzothiazoles (97%), absolute ethanol (99%), and lanthanide nitrate  $[\text{Ln}(\text{NO}_3)_3] \cdot 6\text{H}_2\text{O}$ ,  $\text{Ln}(\text{III}) = \text{La}(\text{III}), \text{Nd}(\text{III}), \text{Er}(\text{III}), \text{Gd}(\text{III}),$  and  $\text{Dy}(\text{III})$  provided by Sigma-Aldrich.

### Instrumentation

The ligand and complexes under investigation underwent microanalysis with a Thermo Finnegan flash device at the Syria Energy Centre. We used a FTIR spectrometer 8400S from Shimadzu, Japan to record the infrared spectra of ligands and their complexes. The spectra covered a range from 4000 to 250  $\text{cm}^{-1}$ . We employed a KBr disk for the ligand and a CsI disk for the complex. In Ankara, Turkey, we recorded the  $^1\text{H}$ -NMR magnetic spectra of the ligands that had been prepared. We employed a Bruker 400 MHz AVANCE spectrometer to analyze the ligands, which were dissolved in  $(\text{DMSO}-d_6)$  solvent. We utilized  $\text{Si}(\text{CH}_3)_4$  as a reference to measure the spectra under room temperature conditions. The University of Ankara in Turkey recorded the mass spectra of the prepared compounds using a network mass-selective device. The Stuart device, manufactured by an English company, was employed to measure the melting points of both the ligand and its complexes. This incredible device features an impressive temperature range of 300  $^\circ\text{C}$ . The University of Baghdad's College of Science for Women hosted the experiment in their Chemistry Department.

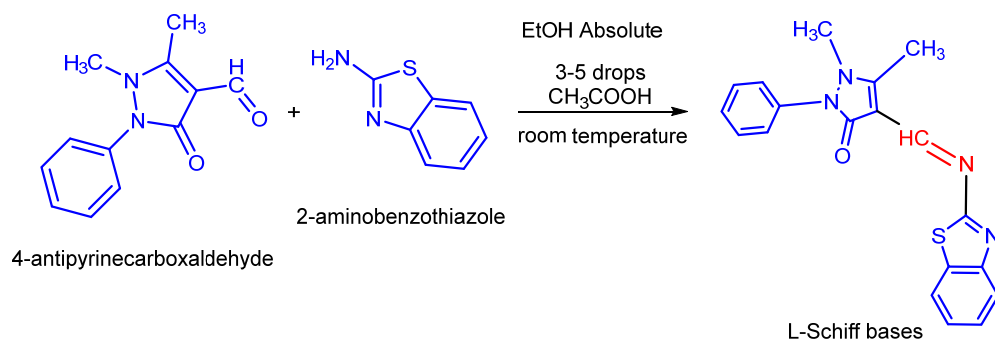
### Procedure

#### Synthesis Schiff base ligand

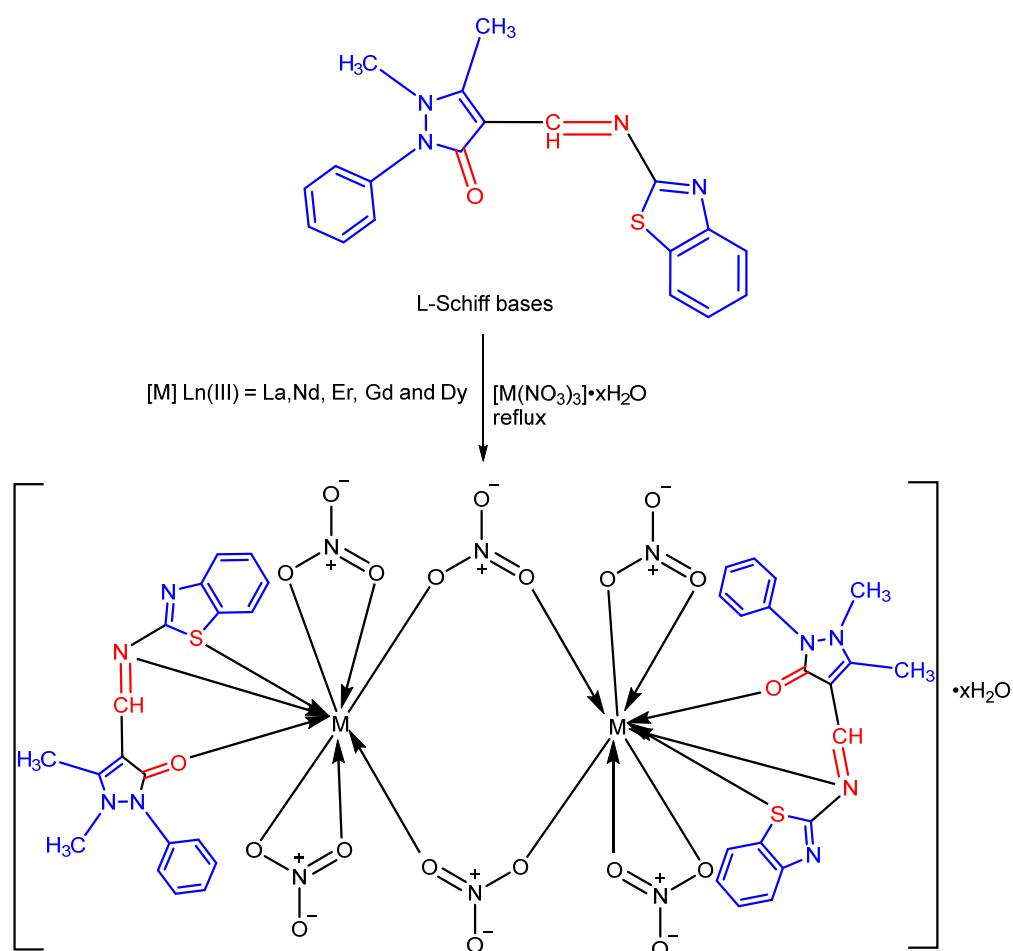
In a 100 mL round-bottom flask, combine 1 g (0.004624 mol) of 4-antipyrinecarboxaldehyde and 0.6945 g (0.004623 mol) of 2-aminobenzothiazol at room temperature, adding 3–5 drops of glacial acetic acid mixed in 20 mL of pure 99.9% ethanol for 1–3 h at a stirring device [29]. After the reaction was complete, the resulting solid was crystallized by absolute ethanol once the reaction was completed. The product was obtained in 70% yield and the melting point of the white crystal was 207–209  $^\circ\text{C}$ .

#### Preparations of complexes

To prepare the complexes, first, dissolve 0.1 g (1 mol) of L-Schiff base in 5 mL of methanol in a 25 mL round bottom flask, and then add 0.1242, 0.1257, 0.1272, 0.1000, and 0.1295 g of salts  $[\text{Ln}(\text{NO}_3)_3] \cdot 6\text{H}_2\text{O}$ ;  $\text{Ln}(\text{III}) = \text{La}(\text{III}), \text{Nd}(\text{III}), \text{Er}(\text{III}), \text{Gd}(\text{III}),$  and  $\text{Dy}(\text{III})$ , respectively,



Scheme 4. Synthesis of L-Schiff bases



Scheme 5. Preparation of Ln(III) complexes

gradually while stirring, 5 mL of an absolute methanol solution and 3–5 drops of acetic acid. The liquid was left to precipitate after having refluxed and stirred for 4–7 h. After collecting the precipitate, it was washed in ether and water and then dried to remove any impurities [30] (Scheme 4 and 5).

### Antibacterial activity

Using the disc diffusion method, the antibacterial activity of the ligand and its complexes was evaluated against *Staphylococcus aureus*, *Bacillus subtilis*, *Escherichia coli*, and *Klebsiella pneumoniae*. In addition, the ligand and its complexes were tested against *Candida*

*albicans*, *Tropical fungi*, and *Scandal fungi*. The disc diffusion method was used to conduct the tests on an agar medium. In order to ensure accurate and reliable results, nutrient agar medium was used, and petri plates were carefully placed. A 5 mm diameter and 1 mm thick disc of glass petri dishes were used to absorb the compounds in DMSO. The discs were placed on microorganism-seeded plates. After an incubation period at 37 °C, we carefully measured the inhibition zone around each disc for bacteria after 24 h and for fungi after 72 h.

## ■ RESULTS AND DISCUSSION

In one step, we prepared Schiff bases using 4-antipyrinecarboxaldehyde and 2-aminobenzothiazole. These Schiff bases were purified by recrystallizing them from absolute ethanol and then undergoing another round of recrystallization for further purification. In the end, we obtained a ligand capable of forming five new complexes through reaction with the appropriate lanthanide nitrate  $[\text{Ln}(\text{NO}_3)_3] \cdot 6\text{H}_2\text{O}$ . The chemical composition of composite materials can be described using various methods, which will be explained in detail in the following sections. Table 1 presents the percentage yields and physical properties of the produced complexes.

### Microanalysis of the Elements

An elemental analysis C, H, N, and X was conducted on the L-Schiff bases and their complexes. The results of these analyses are recorded in Table 1. When comparing the values obtained practically with the values calculated

theoretically, a significant convergence was found between them, which confirms the validity of the added proportions of (m:L), which verifies the accuracy of the proposed formula for the complexes [31]. The physical properties of the prepared element composition of ligand and complexes are presented in Table 1.

### FTIR Spectroscopy of Ligand

By using FTIR spectrum analysis (Fig. S1), Schiff bases compound ( $\text{C}_{19}\text{H}_{16}\text{ON}_4\text{S}$ ) was identified, revealing bands at 3439, 2993, 2860, 1662, 1600 and  $1550\text{ cm}^{-1}$  attributed to O–H, moisture [32], C–H Aliph, C–H Ar, C=O [33], C=N [34], and C=C, respectively.

### <sup>1</sup>H-NMR Spectral of Schiff Bases Ligand

The <sup>1</sup>H-NMR ligand spectra (Fig. S2) exhibit peaks in the DMSO-*d*<sub>6</sub> with a single peak observed at 2.77 ppm for CH<sub>3</sub>. A single peak can be observed at 3.46 ppm in N-CH<sub>3</sub>, various chemical shifts at 7.31 ppm can be seen in C–H, and multiple chemical shifts at 7.54 ppm can be observed in the CH<sub>2</sub> ring of the 4-aminopyrine ring. The signal at 8.8 ppm has been correlated with the proton peak of the azomethine group (CH=N). It was discovered that the 4-aminobenzothiazole ring exhibits multiple signals ranging from 7.9 ppm [35-36].

### Mass Spectral of Ligand

Fig. S3 depicts the LC-mass spectrum; the mass spectra of ligand revealed molecular ion peak at  $348.84\text{ g mol}^{-1}$ , which was in agreement with the calculated value of  $348.42\text{ g mol}^{-1}$  [37].

**Table 1.** Physical properties of microanalysis ligand and lanthanide complexes percentages

Compound	Color	Dec. point (°C)	Yield (%)	Analysis (calculated)					M.wt	M:L
				%C	%H	%N	%O	%S		
$\text{C}_{19}\text{H}_{16}\text{ON}_4\text{S}$ (L)	Yellow	207–209	70%	65.56 (65.50)	4.60 (4.63)	16.06 (16.08)	4.62 (4.59)	9.16 (9.20)	348.42	2:2
$[\text{La}_2\text{L}_2(\text{NO}_3)_6] \cdot 6\text{H}_2\text{O}$	Greenish yellow	260	66%	31.32 (31.37)	3.07 (3.05)	13.49 (13.48)	28.56 (28.59)	4.46 (4.41)	1454.77	2:2
$[\text{Nd}_2\text{L}_2(\text{NO}_3)_6] \cdot 6\text{H}_2\text{O}$	Light yellow	260	60%	31.18 (31.15)	3.00 (3.03)	13.35 (13.38)	28.42 (28.39)	4.36 (4.38)	1465.45	2:2
$[\text{Er}_2\text{L}_2(\text{NO}_3)_6] \cdot 6\text{H}_2\text{O}$	Gold	270	65%	30.23 (30.20)	2.90 (2.93)	12.94 (12.97)	27.54 (27.52)	4.26 (4.24)	1511.48	2:2
$[\text{Gd}_2\text{L}_2(\text{NO}_3)_6] \cdot 6\text{H}_2\text{O}$	Light yellow	260	68%	30.56 (30.60)	2.99 (2.97)	13.18 (13.15)	27.87 (27.89)	4.33 (4.30)	1491.46	2:2
$[\text{Dy}_2\text{L}_2(\text{NO}_3)_6] \cdot 6\text{H}_2\text{O}$	Light yellow	250	65%	30.40 (30.39)	2.93 (2.95)	13.08 (13.06)	27.67 (27.70)	4.30 (4.27)	1501.96	2:2

### FTIR Spectra of Complexes

FTIR spectra of complexes are presented in Fig. S4. Changes in the FTIR spectra of the Ln(III) complexes were observed upon coordination of the Schiff base ligand with the ions Ln(III) = La(III), Nd(III), Er(III), Gd(III), and Dy(III), as shown in Table 2. The spectrum revealed the observation of the C=N stretching absorption peak at wavenumbers 1535, 1519, 1531, 1533, and 1533  $\text{cm}^{-1}$ . The band displayed by this ensemble demonstrates an alteration in both the intensity and location of intricate spectra, suggesting the presence of coordination. Furthermore, the absorption bands at 1666, 1598, 1662, 1664, and 1662  $\text{cm}^{-1}$  can be attributed to the stretching of C=O. The stretching of the M-N bond is responsible for the absorption bands observed at the wavenumbers 430, 408, 428, 430, and 430  $\text{cm}^{-1}$ , respectively. An absorption band is observed at 503, 530, 507, 505, and 505  $\text{cm}^{-1}$  that corresponds to the M-O stretching band. The absorption band at 325, 320, 318, 320, and 324  $\text{cm}^{-1}$  corresponds to the M-S stretching band. The broadband at 3446 to 3342  $\text{cm}^{-1}$  of the spectrum of FTIR spectrum of all produced complexes can be attributed to O-H hydrated water molecules in molecular complex formulas but complex spectra [38-40].

### UV-visible Spectroscopy

Fig. S5 shows the electronic spectrum of the Ln(III) complexes Ln(III) = La, Nd, Er, Gd, and Dy ions in DMF ( $1 \times 10^{-3}$  M) along with the synthesized compounds. It observed that they cannot bond directly because their  $5s^2$  and  $5p^6$  orbitals are well protected. Therefore, ligands mainly do not alter the properties of Ln(III) ions. Ln(III) shows a very sharp electronic spectrum in comparison to

*d*-block metals [41]. Typical lanthanide absorption spectra are derived from  $4f-4f$  transitions, which are analogous to transition metal *d-d* transitions. By contrast with transition metals, lanthanide elements are usually characterized by a sharp, linear spectrum of absorption. Lanthanides are buried deeply within an atom and thus minimize the extended influence of the ligand vibrations [42].

### Magnetic Sensitivity

All electronic distributions for the lanthanide elements, except for the ( $f^0$ ) and ( $f^4$ ) distribute contain individual electrons, and therefore they are described as having a paramagnetic character. The difference between the lanthanide elements and the transition elements is limited to the fact that the magnetic moment of the lanthanide elements does not agree with the spin equation, meaning that the peak does not calculate the equation (Eq. (1)):

$$\mu_{\text{eff}} = 2\sqrt{s[s+1]} \quad (1)$$

In the case of lanthanides, the paramagnetic effect, in addition to the spin movement of the electron, is a result of the magnetic effect caused by the electron's movement in its orbit, meaning that the values of the magnetic moment are calculated from the Eq. (2):

$$\mu_{\text{eff}} = \sqrt{4S[S+1] + L[L-1]} \quad (2)$$

Assessing the magnetic sensitivity of *f*-block constituents poses a significant challenge. The calculation of their  $\mu$  values considers both the spin and orbital contributions, as the  $4f$ -electrons are located Within the  $5s$  and  $5p$  orbitals and exhibit core-like behavior. The magnetic moment values of the Ln(III) complexes reveal that while lanthanum La(III) complexes

**Table 2.** The infrared spectrum reveals the specific positions of the characteristic beams of the L-Schiff bases and its complexes

Symbol of Ln(III) complexes	$\nu(\text{O-H})$ water	$\nu(\text{C=O})$	$\nu(\text{C=N})$	$\nu(\text{NO}_3)$	$\nu(\text{NO}_3)$	$\nu(\text{NO}_3)$	$\nu(\text{NO}_3)$	$\nu(\text{M-O})$	$\nu(\text{M-N})$	$\nu(\text{M-S})$
$\text{cm}^{-1}$										
$\text{C}_{19}\text{H}_{16}\text{ON}_4\text{S}$ (L)	3439	1662	1600	---	---	---	---	---	---	---
$[\text{La}_2\text{L}_2(\text{NO}_3)_6] \cdot 6\text{H}_2\text{O}$	3427	1666	1535	1454	1319	1228	891	503	430	325
$[\text{Nd}_2\text{L}_2(\text{NO}_3)_6] \cdot 6\text{H}_2\text{O}$	3419	1598	1519	1485	1384	1259	920	530	408	320
$[\text{Er}_2\text{L}_2(\text{NO}_3)_6] \cdot 6\text{H}_2\text{O}$	3406	1662	1531	1392	1319	1031	893	507	428	318
$[\text{Gd}_2\text{L}_2(\text{NO}_3)_6] \cdot 6\text{H}_2\text{O}$	3354	1664	1533	1392	1315	1031	893	505	430	320
$[\text{Dy}_2\text{L}_2(\text{NO}_3)_6] \cdot 6\text{H}_2\text{O}$	3433	1662	1533	1390	1311	1029	891	505	430	324

are diamagnetic and the rest are paramagnetic (Table 3). The magnetic moments of the complexes we tested closely correspond to the theoretical values calculated for the free lanthanide Ln(III) ions. Interestingly, these results deviated slightly from the Van Vleck values, suggesting a significant contribution of the 4f electrons in the bonding process [43].

### Molar Conductivity Measurements

Table 3 lists the measured molar conductivity ( $m$ ) of Ln(III) complexes in DMF solutions at 25 °C. All complexes have nitrate ions in the internal coordination domain, as indicated by the  $m$  values falling within the reported range for electrolytes of 1:1 [44-45]. These results are in line with the findings from the discussions on the FTIR and TGA studies below.

### Thermogravimetric analysis

The thermogravimetric analysis (TGA) was performed under a nitrogen atmosphere, with temperatures ranging up to 700 °C and a heating rate of 5 °C/min. The agreement in weight loss between the results obtained from thermal decomposition and the calculated values is evident in Scheme 6, Fig. S6, and Table 4. The ligand along with the lanthanide Ln(III) complexes

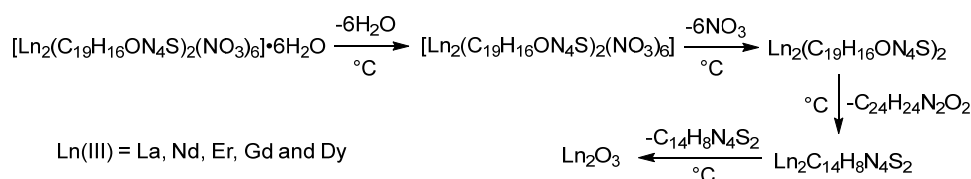
were observed and recorded based on the TGA curve of the ligand. It was observed that it demonstrated three phases of decomposition. The first step of the decomposition of the 2CH<sub>3</sub> groups leads to an estimated mass loss of 9.0% (calculation 8.6%) within the temperature range of 45–150 °C. A loss of approximately 43.2% (calculated as 42.5%) in mass can be expected during the decomposition of the C<sub>7</sub>H<sub>4</sub>N<sub>2</sub>S molecule within the temperature range of 150–425 °C. During the last stage, which ranges from 425 to 585 °C, there was a significant mass reduction of 25.3% (calculated as 26.7%) caused by the complete decomposition of a C<sub>4</sub>HN<sub>2</sub>O molecule [46]. The TGA curves of Ln(III) = La, Nd, Er, Gd, and Dy, showed four decomposition steps, as shown in Table 4.

### Schiff Bases as Antimicrobial Agents

Most diseases that affect humans and animals are caused by microscopic objects, and the discovery of chemical therapeutic agents has played an important role in controlling and preventing these diseases. Chemical treatments come from many sources. The source of chemical compounds is created by chemists. The C=N compounds are highly effective at inhibiting a

**Table 3.** The UV-vis, magnetic susceptibility measurements, and other physical properties of ligand and its complexes Ln(III) in DMF solvent at  $1 \times 10^{-3}$  M concentration

Compound	Configuration Ln(III) (No. of unpaired e-)	Conductivity DMF (cm <sup>2</sup> ohm <sup>-1</sup> mol <sup>-1</sup> )	Absorption bonds (nm)	Ground state	Assigned transition	Magnetic susceptibility (B.M)	$\mu$ J B.M
C <sub>19</sub> H <sub>16</sub> ON <sub>4</sub> S (L)	---	---	242, 385, 920	---	$n \rightarrow \pi^*$ , $\pi \rightarrow \pi^*$	---	---
[La <sub>2</sub> L <sub>2</sub> (NO <sub>3</sub> ) <sub>6</sub> ].6H <sub>2</sub> O	4f <sup>0</sup> (0)	16	---	<sup>1</sup> S <sub>0</sub>	<sup>1</sup> S <sub>0</sub>	Dia	---
[Nd <sub>2</sub> L <sub>2</sub> (NO <sub>3</sub> ) <sub>6</sub> ].6H <sub>2</sub> O	4f <sup>3</sup> (3)	24	582, 891, 918, 950	<sup>4</sup> I <sub>9/2</sub>	<sup>4</sup> I <sub>9/2</sub> → <sup>4</sup> G <sub>7/2</sub> , <sup>4</sup> I <sub>9/2</sub> → <sup>2</sup> D <sub>7/2</sub> , <sup>4</sup> I <sub>9/2</sub> → <sup>2</sup> P <sub>1/2</sub>	4.59	3.62
[Er <sub>2</sub> L <sub>2</sub> (NO <sub>3</sub> ) <sub>6</sub> ].6H <sub>2</sub> O	4f <sup>11</sup> (3)	30	487, 521, 541, 652, 803	<sup>4</sup> I <sub>15/2</sub>	<sup>4</sup> I <sub>15/2</sub> → <sup>4</sup> I <sub>15/2</sub> , <sup>4</sup> I <sub>15/2</sub> → <sup>4</sup> G <sub>11/2</sub>	2.09	9.60
[Gd <sub>2</sub> L <sub>2</sub> (NO <sub>3</sub> ) <sub>6</sub> ].6H <sub>2</sub> O	4f <sup>7</sup> (7)	25	758, 808, 914	<sup>8</sup> S <sub>7/2</sub>	<sup>8</sup> S <sub>7/2</sub> → <sup>6</sup> I <sub>7/2</sub>	2.97	7.94
[Dy <sub>2</sub> L <sub>2</sub> (NO <sub>3</sub> ) <sub>6</sub> ].6H <sub>2</sub> O	4f <sup>9</sup> (5)	27	621, 636, 814, 920	<sup>6</sup> H <sub>15/2</sub>	<sup>6</sup> H <sub>5/2</sub> → <sup>5</sup> I <sub>11</sub> , <sup>6</sup> H <sub>15/2</sub> → <sup>6</sup> P <sub>5/2</sub>	4.02	10.60



**Scheme 6.** TGA of Ln(III) complexes

**Table 4.** TGA data of L-Schiff bases and its Ln(III) complexes

Sample (step)	Temp. range (°C)	Weight mass loss		Reaction	Sample (step)	Temp. range (°C)	Weight mass loss		Reaction
		Calc%	Found%				Calc%	Found%	
L <sub>(I)</sub>	45–150	8.6	9.0	2(CH <sub>3</sub> )	Er <sub>(I)</sub>	25–80	7.1	6.5	6(H <sub>2</sub> O)
L <sub>(II)</sub>	150–425	42.5	43.2	C <sub>7</sub> H <sub>4</sub> N <sub>2</sub> S	Er <sub>(II)</sub>	80–255	24.6	23.9	6(NO <sub>3</sub> )
L <sub>(III)</sub>	425–585	26.7	25.3	C <sub>4</sub> H <sub>2</sub> N <sub>2</sub> O	Er <sub>(III)</sub>	255–462	26.4	27.2	C <sub>24</sub> H <sub>24</sub> N <sub>4</sub> O <sub>2</sub>
Final residual		22.1	22.5	C <sub>6</sub> H <sub>5</sub>	Er <sub>(IV)</sub>	462–545	19.6	20.1	C <sub>14</sub> H <sub>8</sub> N <sub>4</sub> S <sub>2</sub>
La <sub>(I)</sub>	35–97	7.4	8.0	6(H <sub>2</sub> O)	Final residual		25.3	22.3	Er <sub>2</sub> O <sub>3</sub>
La <sub>(II)</sub>	97–256	25.5	24.9	6(NO <sub>3</sub> )	Gd <sub>(I)</sub>	25–90	7.2	6.8	6(H <sub>2</sub> O)
La <sub>(III)</sub>	256–450	27.5	26.7	C <sub>24</sub> H <sub>24</sub> N <sub>4</sub> O <sub>2</sub>	Gd <sub>(II)</sub>	90–275	24.9	25.5	6(NO <sub>3</sub> )
La <sub>(IV)</sub>	450–535	20.3	21.1	C <sub>14</sub> H <sub>8</sub> N <sub>4</sub> S <sub>2</sub>	Gd <sub>(III)</sub>	275–478	26.8	27.0	C <sub>24</sub> H <sub>24</sub> N <sub>4</sub> O <sub>2</sub>
Final residual		22.3	19.3	La <sub>2</sub> O <sub>3</sub>	Gd <sub>(IV)</sub>	478–560	19.8	19.4	C <sub>14</sub> H <sub>8</sub> N <sub>4</sub> S <sub>2</sub>
Nd <sub>(I)</sub>	30–85	7.3	8.2	6(H <sub>2</sub> O)	Final residual		24.3	21.3	Gd <sub>2</sub> O <sub>3</sub>
Nd <sub>(II)</sub>	85–264	25.3	24.7	6(NO <sub>3</sub> )	Dy <sub>(I)</sub>	20–70	7.1	6.8	6(H <sub>2</sub> O)
Nd <sub>(III)</sub>	264–445	27.3	28.7	C <sub>24</sub> H <sub>24</sub> N <sub>4</sub> O <sub>2</sub>	Dy <sub>(II)</sub>	70–245	24.7	23.6	6(NO <sub>3</sub> )
Nd <sub>(IV)</sub>	445–540	20.2	18.5	C <sub>14</sub> H <sub>8</sub> N <sub>4</sub> S <sub>2</sub>	Dy <sub>(III)</sub>	245–455	26.6	27.4	C <sub>24</sub> H <sub>24</sub> N <sub>4</sub> O <sub>2</sub>
Final residual		22.9	19.9	Nd <sub>2</sub> O <sub>3</sub>	Dy <sub>(IV)</sub>	455–550	19.7	19.4	C <sub>14</sub> H <sub>8</sub> N <sub>4</sub> S <sub>2</sub>
					Final residual		24.8	21.9	Dy <sub>2</sub> O <sub>3</sub>

wide range of pathogenic bacteria and fungi. Their solutions dissolve the cell's outer wall, causing fluids within the cell to exude and kill the cell. There are effective aggregates, such as hybrid corn within the composition of the biologically active ligand, the C=N derivative. It is the nitrogen that qualifies it to bind with the various elements in the cell body that the bacterial cell requires: La(III), Nd(III), Gd(III), Er(III), and Dy(III) ions, resulting in the formation of complexes with these elements and thus cell death due to the loss of these elements to study the effect of the biological activity of the ligand and its complexes prepared with its ions [39,47].

The effect of the biological activity of ligand and its complexes prepared with ions (La(III), Nd(III), Gd(III), Er(III), and Dy(III)) was studied. Four types of pathogenic bacteria were used; these bacteria are *S. aureus* and *B. subtilis*, representative of the positive bacteria while *E. coli*

and *K. pneumonia* represent Gram-negative bacteria. The drilling method (wells) was adopted in calculating the inhibitory or lethal effect, as it included making three holes with a diameter of 6 mm by a drill cork, and then the damping diameter was measured with a ruler, where the bacterial growth process occurred in the Hinton-Mueller agar media at room temperature for 24 h. The inhibition results were included in Table 5 and Fig. S7, where we note that the prepared metal compounds affect the biological activity of bacteria *S. aureus* except the La(III) complex, while we note that the ligand and its prepared metal complexes have high activity and sensitivity towards the biological activity of *K. pneumoniae* bacteria. As for the metal complexes prepared from the ligand, they affect the biological activity of *B. subtilis* bacteria except for the Dy(III) complex, and it is noted that the ligand and its complexes

**Table 5.** The effect of ligand and its complexes dissolved in DMSO at a concentration of  $1 \times 10^{-3}$  M on four types of pathogenic bacteria

Sample	<i>S. aureus</i> <i>B. subtilis</i> <i>E. coli</i> <i>K. pneumoniae</i>			
	mm			
C <sub>19</sub> H <sub>16</sub> ON <sub>4</sub> S (L)	26	24	21	27
[La <sub>2</sub> L <sub>2</sub> (NO <sub>3</sub> ) <sub>6</sub> ]-6H <sub>2</sub> O	20	22	21	28
[Nd <sub>2</sub> L <sub>2</sub> (NO <sub>3</sub> ) <sub>6</sub> ]-6H <sub>2</sub> O	26	25	18	34
[Er <sub>2</sub> L <sub>2</sub> (NO <sub>3</sub> ) <sub>6</sub> ]-6H <sub>2</sub> O	30	29	20	31
[Gd <sub>2</sub> L <sub>2</sub> (NO <sub>3</sub> ) <sub>6</sub> ]-6H <sub>2</sub> O	33	30	24	30
[Dy <sub>2</sub> L <sub>2</sub> (NO <sub>3</sub> ) <sub>6</sub> ]-6H <sub>2</sub> O	31	20	25	27

**Table 6.** The effect of ligand and its complexes dissolved in DMSO at a concentration of  $1 \times 10^{-3}$  M on three types of fungi

Sample	<i>C. tropical</i>	<i>C. scandal</i>	<i>C. albicans</i>
	mm		
C <sub>19</sub> H <sub>16</sub> ON <sub>4</sub> S (L)	10	9	10
[La <sub>2</sub> L <sub>2</sub> (NO <sub>3</sub> ) <sub>6</sub> ].6H <sub>2</sub> O	12	13	14
[Nd <sub>2</sub> L <sub>2</sub> (NO <sub>3</sub> ) <sub>6</sub> ].6H <sub>2</sub> O	11	10	11
[Er <sub>2</sub> L <sub>2</sub> (NO <sub>3</sub> ) <sub>6</sub> ].6H <sub>2</sub> O	11	12	14
[Gd <sub>2</sub> L <sub>2</sub> (NO <sub>3</sub> ) <sub>6</sub> ].6H <sub>2</sub> O	11	11	15
[Dy <sub>2</sub> L <sub>2</sub> (NO <sub>3</sub> ) <sub>6</sub> ].6H <sub>2</sub> O	12	10	15

had less biological activity with *E. coli* except for the Gd(III) and Dy(III) complexes [48-51].

### Schiff Bases with Antifungal Activities

An *in vitro* test was conducted to assess the antifungal activity of Schiff base ligand complexed with metal complexes Ln(III) such as La(III), Nd(III), Er(III), Gd(III), and Dy(III) at a concentration of  $1 \times 10^{-3}$  M and the result is shown in Table 6. The results showed that *C. albicans* gave more efficacy compared to *Tropical fungi* and *Scandal fungi* under identical experimental conditions. The results show that the ligand and its complexes inhibit *C. albicans* fungi strongly under the test conditions. As compared with their parent ligands and under identical experimental conditions, the complexes are more toxic and exhibit strong antifungal activity against the three selected fungi, except for the ligand. The metal ion may enhance the antifungal activity of metal chelates by affecting the normal cell process [52]. Because of the partial sharing of the positive charge by the donor groups and the possibility of *p*-electron delocalization over the entire chelate ring, chelation reduces the polarity of the metal ion considerably. Through such chelation, the central metal atom becomes more lipophilic, which facilitates its permeation through the lipid layers of cell membranes. In addition, the compounds may interfere with the normal function of cells by forming hydrogen bonds with the active centers of cell constituents through the C=N group [53], as shown in Fig. S8.

### CONCLUSION

The synthesis and characterization of Ln(III) = La, Nd, Er, Gd, and Dy complexes of the Schiff base ligand produced via the condensation reaction of 4-

antipyrinecarboxaldehyde with 2-aminobenzothiazole are reported in this study. Various analytical and spectroscopic techniques, including elemental analysis, FTIR, <sup>1</sup>H-NMR, UV-vis, and TGA analysis, were used to completely elucidate the synthesized ligand and complexes. Metal complexes' molar conductance value demonstrates their non-electrolytic nature. At room temperature, the complexes were shown to be stable. Based on the spectroscopic results, the data clearly indicate that the complexes have a composition of a certain type. Based on spectroscopic data, it can be concluded that the central metal ion is a binuclear unit. All complexes are coordinated to 14 oxygen atoms (12 from the nitrate and two from the antipyrine ligand), and it is considered one of the strongest electron donor atoms, forming covalent bonds with the lanthanide atom, two azomethine nitrogen and two sulfur atoms from the 2-aminobenzothiazole ligand. Biologically, the complexes were effective against a variety of bacteria and fungi.

### ACKNOWLEDGMENTS

Our sincere appreciation goes out to the Department of Chemistry, College of Science for Women, University of Baghdad, Iraq, for its support. Chemicals and research equipment have been provided by them.

### AUTHOR CONTRIBUTIONS

The idea was conceived by Naser Shaalan based on Kawther Adeeb Hussein's expressions. The experiment was carried out, the manuscript was written, and the analysis was performed by Kawther Adeeb Hussein. The final manuscript was drafted by all authors after a discussion of the results.

## ■ REFERENCES

- [1] Cotton, S., 2013, Lanthanide and actinide chemistry, John Wiley & Sons, Hoboken, New Jersey, US.
- [2] Gupta, I., Singh, S., Bhagwan, S., and Singh, D., 2021, Rare earth (RE) doped phosphors and their emerging applications: A review, *Ceram. Int.*, 47 (14), 19282–19303.
- [3] Wang, C., 2023, *Theory and Application of Rare Earth Materials*, Springer Singapore, Singapore.
- [4] Cossard, A., Desmarais, J.K., Casassa, S., Gatti, C., and Erba, A., 2021, Charge density analysis of actinide compounds from the quantum theory of atoms in molecules and crystals, *J. Phys. Chem. Lett.*, 12 (7), 1862–1868.
- [5] Vernon, R.E., 2021, The location and composition of group 3 of the periodic table, *Found. Chem.*, 23 (2), 155–197.
- [6] Paderni, D., Giorgi, L., Fusi, V., Formica, M., Ambrosi, G., and Micheloni, M., 2021, Chemical sensors for rare earth metal ions, *Coord. Chem. Rev.*, 429, 213639.
- [7] Liu, Y., 2021, Durabilité des revêtements de barrière thermique pulvérisé au plasma atmosphérique dopés aux terres rares pour le diagnostic thermique et structurel, *Dissertation*, Institut Supérieur de l'Aéronautique et de l'Espace, Toulouse, France.
- [8] Salman, A.D., Juzsakova, T., Mohsen, S., Abdullah, T.A., Le, P.C., Sebestyen, V., Sluser, B., and Cretescu, I., 2022, Scandium recovery methods from mining, metallurgical extractive industries, and industrial wastes, *Materials*, 15 (7), 2376.
- [9] Razavi, R., and Amiri, M., 2022, "Rare earth-based ceramic nanomaterials—manganites, ferrites, cobaltites, and nickelates" in *Advanced Rare Earth-Based Ceramic Nanomaterials*, Eds. Zinatloo-Ajabshir, S., Elsevier, Amsterdam, Netherlands, 205–230.
- [10] Patil, A.S., Patil, A.V., Dighavkar, C.G., Adole, V.A., and Tupe, U.J., 2022, Synthesis techniques and applications of rare earth metal oxides semiconductors: A review, *Chem. Phys. Lett.*, 796, 139555.
- [11] Bünzli, J.C.G., 2016, "Chapter 287 - Lanthanide Luminescence: From a Mystery to Rationalization, Understanding, and Applications" in *Handbook on the Physics and Chemistry of Rare Earths*, Vol. 50, Eds., Bünzli, J.C.G., and Pecharsky, V.K., Elsevier, Amsterdam, Netherlands, 141–176.
- [12] Koper, G.H.M., and Terpstra, M., 2012, *Improving the Properties of Permanent Magnets: A Study of Patents, Patent Applications and Other Literature*, Springer Dordrecht, Berlin, Germany.
- [13] Wang, K., Han, C., Shao, Z., Qiu, J., Wang, S., and Liu, S., 2021, Perovskite oxide catalysts for advanced oxidation reactions, *Adv. Funct. Mater.*, 31 (30), 2102089.
- [14] Maity, U.K., Manoravi, P., Joseph, M., and Sivaraman, N., 2022, Laser-induced breakdown spectroscopy for simultaneous determination of lighter lanthanides in actinide matrix in aqueous medium, *Spectrochim. Acta, Part B*, 190, 106393.
- [15] Aaseth, J., and Berlinger, B., 2022, "Lanthanum" in *Handbook on the Toxicology of Metals*, 5<sup>th</sup> Ed., Eds. Nordberg, G.F., and Costa, M., Academic Press, Cambridge, Massachusetts, US, 419–425.
- [16] Hasan, M.M., Bithe, S.A., Neher, B., and Ahmed, F., 2022, Polythiophene as a sensor model for chlorofluorocarbon, fluorine, and oxygen gas using DFT calculations, *J. Mol. Model.*, 28 (3), 59.
- [17] Arnold, B., 2022, *Zircon, Zirconium, Zirconia-Similar Names, Different Materials*, Springer Berlin, Heidelberg, Germany.
- [18] Hasegawa, M., Ohmagari, H., Tanaka, H., and Machida, K., 2022, Luminescence of lanthanide complexes: From fundamental to prospective approaches related to water- and molecular-stimuli, *J. Photochem. Photobiol., C*, 50, 100484.
- [19] Lima, A.T., Kirkelund, G.M., Ntuli, F., and Ottosen, L.M., 2022, Rare earth elements extractability from residual waste materials, *Proceedings of the 9<sup>th</sup> International Conference on Engineering for Waste and Biomass Valorisation*, Technical University of Denmark, Copenhagen, Denmark, 27-30 July 2022, 699–700.
- [20] Krüger, L., 2020, "Rare Earth Elements—A Treasure Locked in AMD?" in *Recovery of Byproducts from Acid Mine Drainage Treatment*, Eds Fosso-Kankeu, E., Wolkersdorfer, C., and Burges, J., John Wiley & Sons, Inc., Hoboken, NJ, US, 263–313.

- [21] Jin, S., Li, R., Huang, H., Jiang, N., Lin, J., Wang, S., Zheng, Y., Chen, X., and Chen, D., 2022, Compact ultrabroadband light-emitting diodes based on lanthanide-doped lead-free double perovskites, *Light: Sci. Appl.*, 11 (1), 52.
- [22] Lei, Y.H., Jiang, J.H., Li, X., Li, Q.G., and Li, C.H., 2022, A nine-coordinated bismuth(III) Schiff-base complex: Design, synthesis, computational studies, and antimicrobial activity, *Appl. Organomet. Chem.*, 36 (2), e6523.
- [23] Shahi, S., Roghani-Mamaqani, H., Talebi, S., and Mardani, H., 2022, Chemical stimuli-induced reversible bond cleavage in covalently crosslinked hydrogels, *Coord. Chem. Rev.*, 455, 214368.
- [24] Troschke, E., Oschatz, M., and Ilic, I.K., 2021, Schiff-bases for sustainable battery and supercapacitor electrodes, *Exploration*, 1 (3), 20210128.
- [25] Faujdar, E., and Singh, R.K., 2021, Study on alkylated Schiff base of a triazole with 3,5-di-tert-butyl-4-hydroxybenzaldehyde as a novel multifunctional lubricant additive, *Fuel*, 302, 121158.
- [26] Akagawa, M., 2021, Protein carbonylation: Molecular mechanisms, biological implications, and analytical approaches, *Free Radical Res.*, 55 (4), 307–320.
- [27] Fuentes-Lemus, E., Häggglund, P., López-Alarcón, C., and Davies, M.J., 2021, Oxidative crosslinking of peptides and proteins: Mechanisms of formation, detection, characterization and quantification, *Molecules*, 27 (1), 15.
- [28] Battin, S.N., 2019, *Vanillin-Aminoquinoline Schiff Bases and their Co(II), Ni(II) and Cu(II) Complexes*, Lulu Press, Inc., Morrisville, North Carolina, US.
- [29] Hussein, K.A., and Shaalan, N., 2022, Synthesis, characterization, and antibacterial activity of lanthanide metal complexes with Schiff base ligand produced from reaction of 4,4-methylene diantipyrene with ethylenediamine, *Indones. J. Chem.*, 22 (5), 1365–1375.
- [30] Hussein, K.A., Mahdi, S., and Shaalan, N., 2023, Synthesis, spectroscopy of new lanthanide complexes with Schiff base derived from (4-antipyrene carboxaldehyde with ethylene di-amine) and study the bioactivity, *Baghdad Sci. J.*, 20 (2), 305–305.
- [31] Hammada, R.G., and Shaalan, N., 2023, Synthesis of Zn(II) and Co(II) complexes with a Schiff base derived from malonic acid dihydrazide for photo-stabilizers of polystyrene, *Indones. J. Chem.*, 23 (5), 1324–1340.
- [32] Taha, Z.A., Ajlouni, A.M., Al-Hassan, K.A., Hijazi, A.K., and Faiq, A.B., 2011, Syntheses, characterization, biological activity, and fluorescence properties of bis-(salicylaldehyde)-1, 3-propylenediimine Schiff base ligand and its lanthanide complexes, *Spectrochim. Acta, Part A*, 81 (1), 317–323.
- [33] Nandiyanto, A.B.D., Ragadhita, R., and Fiandini, M., 2023, Interpretation of Fourier transforms infrared spectra (FTIR): A practical approach in the polymer/plastic thermal decomposition, *Indones. J. Sci. Technol.*, 8 (1), 113–126.
- [34] Kariaka, N.S., Kolotilov, S.V., Gawryszewska, P., Kasprzycka, E., Weselski, M., Dyakonenko, V.V., Shishkina, S.V., Trush, V.A., and Amirkhanov, V.M., 2019, Structures and spectral and magnetic properties of a series of carbacylamidophosphate pentanuclear lanthanide(III) hydroxo complexes, *Inorg. Chem.*, 58 (21), 14682–14692.
- [35] Teran, R., Guevara, R., Mora, J., Dobronski, L., Barreiro-Costa, O., Beske, T., Pérez-Barrera, J., Araya-Maturana, R., Rojas-Silva, P., Poveda, A., and Heredia-Moya, J., 2019, Characterization of antimicrobial, antioxidant, and leishmanicidal activities of Schiff base derivatives of 4-aminoantipyrene, *Molecules*, 24 (15), 2696.
- [36] Al-Shaheen, A.J., and Al-Bergas, A.F., 2020, Synthesis and identification of some complexes of 4-[N-(2,4-dihydroxybenzylidene) imino] antipyrynyl with serine (L1) or with theronine (L2) ligands and evaluation of their bacteria activities, *J. Educ. Sci.*, 29 (4), 42–61.
- [37] Niessen, W.M., and Falck, D., 2015, “Introduction to Mass Spectrometry, a Tutorial” in *Analyzing Biomolecular Interactions by Mass Spectrometry*, Eds. Kool, J., and Niessen, W.M.A., Wiley-VCH Verlag GmbH & Co. KGaA, Weinheim, Germany, 1–54.

- [38] Hassan, S.A., Lateef, S.M., and Majeed, I.Y., 2020, Structural, spectral and thermal studies of new bidentate Schiff base ligand type (NO) derived from mebendazol and 4-aminoantipyrine and it's metal complexes and evaluation of their biological activity, *Res. J. Pharm. Technol.*, 13 (6), 3001–3006.
- [39] Hussein, K.A., and Shaalan, N., 2021, Synthesis, spectroscopy and biological activities studies for new complexes of some lanthanide metals with Schiff's bases derived from dimedone with 4-aminoantipyrine, *Chem. Methodol.*, 6 (2), 103–113.
- [40] Cruz-Navarro, A., Rivera, J.M., Durán-Hernández, J., Castillo-Blum, S., Flores-Parra, A., Sánchez, M., Hernández-Ahuactzi, I., and Colorado-Peralta, R., 2018, Luminescence properties and DFT calculations of lanthanide(III) complexes (Ln= La, Nd, Sm, Eu, Gd, Tb, Dy) with 2,6-bis(5-methyl-benzimidazol-2-yl) pyridine, *J. Mol. Struct.*, 1164, 209–216.
- [41] Anonymous, 2021, *Physical Chemistry (LibreTexts)*, <https://chem.libretexts.org/@go/page/9054>, accessed January 31, 2022.
- [42] Ferenc, W., Sadowski, P., Cristóvão, B., and Sarzyński, J., 2013, Investigation of some physicochemical properties of 4-nitrocinnamates of lanthanides(III), *J. Chil. Chem. Soc.*, 58 (2), 1753–1758.
- [43] Sorace, L., and Gatteschi, D., 2015, “Electronic Structure and Magnetic Properties of Lanthanide Molecular Complexes” in *Lanthanides and Actinides in Molecular Magnetism*, Wiley-VCH Verlag GmbH & Co. KGaA, Weinheim, Germany, 1–26.
- [44] Hussain, A., Gadadhar, S., Goswami, T.K., Karande, A.A., and Chakravarty, A.R., 2012, Photo-induced DNA cleavage activity and remarkable photocytotoxicity of lanthanide(III) complexes of a polypyridyl ligand, *Dalton Trans.*, 41 (3), 885–895.
- [45] Abbas, A.K., 2016, Preparation, characterization and biological evaluation of some lanthanide(III) ions complexes with 3-(1-methyl-2-benzimidazolylazo)-tyrosine, *Baghdad. Sci. J.*, 13 (2), 128–128.
- [46] Zhang, F., Huang, F., Yao, X., Jin, Y., Chen, Q., Liu, F., and Li, G., 2015, Pyridine carboxylate lanthanide coordination complexes with 1D and 2D structure, *J. Inorg. Organomet. Polym. Mater.*, 25 (5), 1183–1188.
- [47] Obaid, S.M.H., Jarad, A.J., and Salih Al-Hamdani, A.A., 2020, Synthesis, characterization and biological activity of mixed ligand metal salts complexes with various ligands, *J. Phys.: Conf. Ser.*, 1660 (1), 012028.
- [48] Holland, N., Pang, X., Herzberg, W., Bor, J., and Lorenz, E., 2021, Combination of physics based simulation and machine learning for PV power forecasting of large power plants, *The 38<sup>th</sup> European Photovoltaic Solar Energy Conference and Exhibition (EU PVSEC)*, Lisbon, Portugal, 6-10 September 2021.
- [49] Shaalan, N., 2022, Preparation, spectroscopy, biological activities and thermodynamic studies of new complexes of some metal ions with 2-[5-(2-hydroxy-phenyl)-1,3,4-thiadiazol-2-ylimino]-methyl-naphthalen-1-ol], *Baghdad Sci. J.*, 19 (4), 829–829.
- [50] Shaalan, N.D., and Abdulwahhab, S., 2021, Synthesis, characterization and biological activity study of some new metal complexes with Schiff's bases derived from [*o*-vanillin] with [2-amino-5-(2-hydroxy-phenyl)-1,3,4-thiadiazole], *Egypt. J. Chem.*, 64 (8), 4059–4067.
- [51] Shaalan, N., Khalaf, W.M., and Mahdi, S., 2022, Preparation and characterization of new tetradentate N<sub>2</sub>O<sub>2</sub> Schiff base with some of metal ions complexes, *Indones. J. Chem.*, 22 (1), 62–71.
- [52] Jarrahpour, A.A., Motamedifar, M., Pakshir, K., Hadi, N., and Zarei, M., 2004, Synthesis of novel azo Schiff bases and their antibacterial and antifungal activities, *Molecules*, 9 (10), 815–824.
- [53] Wang, C., Fan, L., Pan, Z., Fan, S., Shi, L., Li, X., Zhao, J., Wu, L., Yang, G., and Xu, C., 2022, Synthesis of novel indole Schiff base compounds and their antifungal activities, *Molecules*, 27 (20), 6858.